AD-A062 133 AIR FORCE AVIONICS LAB WRIGHT-PATTERSON AFB OHIO F/G 9/1
THERMAL CYCLING ANALYSIS OF THE THERMOPLASTIC MODULATOR.(U)
JUL 78 D L FLANNERY

UNCLASSIFIED AFAL-TR-78-102 NL

1 OF 1
AD
A062 133

END
DATE FILMED
3-79
DDC

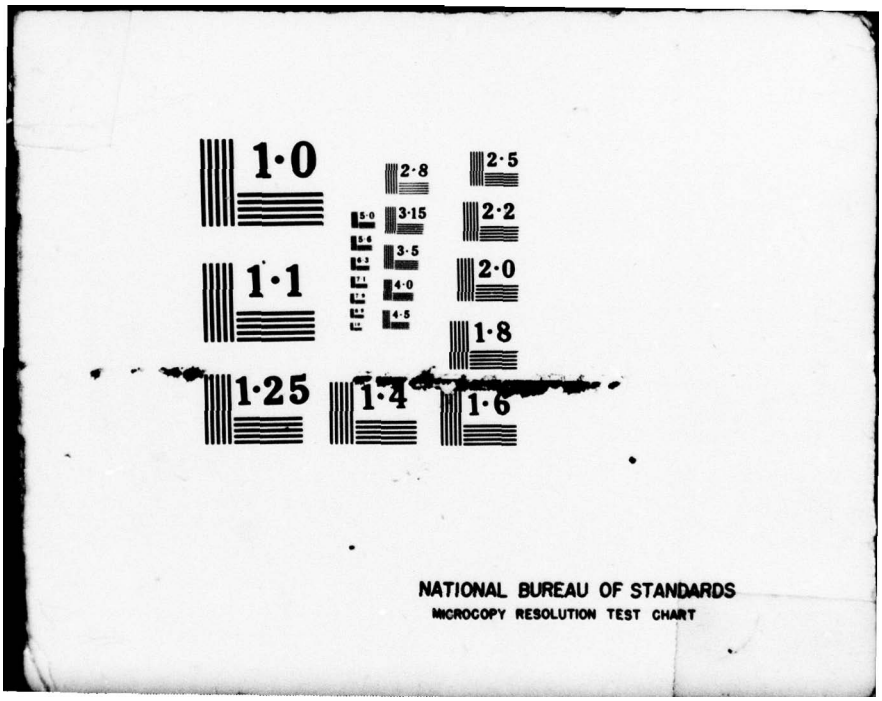
1·0
1·1
1·25
2·8
3·15
3·5
4·0
4·5
5·0
2·5
2·2
2·0
1·8
1·4
1·6
NATIONAL BUREAU OF STANDARDS
MICROCOPY RESOLUTION TEST CHART

AFAL-TR-78-102

LEVEL II

THERMAL CYCLING ANALYSIS OF THE THERMOPLASTIC MODULATOR

Electro-Optics Technology Branch
Electronic Technology Division

July 1978

TECHNICAL REPORT AFAL-TR-78-102

Interim Report for Period October 1977 - March 1978

AIR FORCE AVIONICS LABORATORY
AIR FORCE WRIGHT AERONAUTICAL LABORATORIES
AIR FORCE SYSTEMS COMMAND
WRIGHT-PATTERSON AIR FORCE BASE, OHIO 45433

NOTICE

When Government drawings, specifications, or other data are used for any purpose other than in connection with a definitely related Government procurement operation, the United States Government thereby incurs no responsibility nor any obligation whatsoever; and the fact that the government may have formulated, furnished, or in any way supplied the said drawings, specifications, or other data, is not to be regarded by implication or otherwise as in any manner licensing the holder or any other person or corporation, or conveying any rights or permission to manufacture, use, or sell any patented invention that may in any way be related thereto.

This report has been reviewed by the Information Office (OI) and is releasable to the National Technical Information Service (NTIS). At NTIS, it will be available to the general public, including foreign nations.

This technical report has been reviewed and is approved for publication.

David L. Flannery

DAVID L. FLANNERY
Project Engineer

Kenneth R. Hutchinson

KENNETH R. HUTCHINSON
Chief
E-O Techniques and Applications Grp

FOR THE COMMANDER

Ronald F. Paulson

RONALD F. PAULSON, Acting Chief
Electro-Optics Technology Branch
Electronic Technology Division

"If your address has changed, if you wish to be removed from our mailing list, or if the addressee is no longer employed by your organization please notify AFAL/DHO ,W-PAFB, OH 45433 to help us maintain a current mailing list".

Copies of this report should not be returned unless return is required by security considerations, contractual obligations, or notice on a specific document.

UNCLASSIFIED

SECURITY CLASSIFICATION OF THIS PAGE (When Data Entered)

REPORT DOCUMENTATION PAGE

READ INSTRUCTIONS BEFORE COMPLETING FORM

1. REPORT NUMBER: AFAL-TR-78-192	2. GOVT ACCESSION NO.
3. RECIPIENT'S CATALOG NUMBER: rept.	
4. TITLE (and Subtitle): THERMAL CYCLING ANALYSIS OF THE THERMOPLASTIC MODULATOR.	5. TYPE OF REPORT & PERIOD COVERED: Interim, Oct 77 - Mar 78
	6. PERFORMING ORG. REPORT NUMBER
7. AUTHOR(s): David L. Flannery	8. CONTRACT OR GRANT NUMBER(s)
9. PERFORMING ORGANIZATION NAME AND ADDRESS: Electro-Optics Technology Branch (DHO) Air Force Avionics Laboratory Wright-Patterson Air Force Base, Ohio 45433	10. PROGRAM ELEMENT, PROJECT, TASK AREA & WORK UNIT NUMBERS: Project No. 2001 Task No. 200102 62204F Work Unit 20010246
11. CONTROLLING OFFICE NAME AND ADDRESS: Air Force Avionics Laboratories Wright-Patterson Air Force Base, Ohio 45433	12. REPORT DATE: July 78 13. NUMBER OF PAGES: 45
14. MONITORING AGENCY NAME & ADDRESS (if different from Controlling Office): 12 48p.	15. SECURITY CLASS. (of this report): Unclassified 15a. DECLASSIFICATION/DOWNGRADING SCHEDULE

16. DISTRIBUTION STATEMENT (of this Report)

Approved for public release; distribution unlimited.

17. DISTRIBUTION STATEMENT (of the abstract entered in Block 20, if different from Report)

18. SUPPLEMENTARY NOTES

19. KEY WORDS (Continue on reverse side if necessary and identify by block number)

Thermal cycling
Heat removal
Electro-Optics
Coherent optical processing

20. ABSTRACT (Continue on reverse side if necessary and identify by block number)

The problem of heat removal from the faceplate of a Thermoplastic Modulator for Coherent Optical Processing during rapid write-erase cycling was analyzed using two complementary theoretical approaches. Pertinent cases were treated and important results, having bearing on future designs, were obtained. Also, three likely candidates for substrate-to-ambient cooling were compared with the result that only one seems feasible.

DD FORM 1 JAN 73 1473 EDITION OF 1 NOV 65 IS OBSOLETE

Unclassified

SECURITY CLASSIFICATION OF THIS PAGE (When Data Entered)

FOREWORD

The interim report was prepared in the Electro-Optics Technology Branch (DHO) of the Air Force Avionics Laboratory, Wright-Patterson Air Force Base, Ohio. The work was conducted under Project No. 2001 "Electro-Optics Technology," Task No. 200102 "Light Control Devices," Work Unit No. 20010246 "Thermoplastic Modulator Development." The time period covered was October 1977 - March 1978. This analysis was done to supplement the work effort of Contract F 33615-77-C-1019 performed at the Environmental Research Institute of Michigan. The final report on the contract effort is AFAL-TR-78-86.

N.H.)

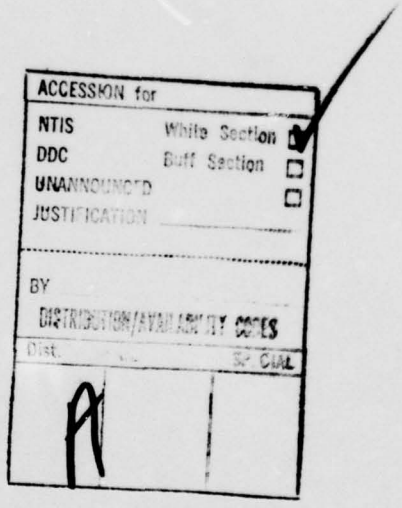

TABLE OF CONTENTS

LIST OF ILLUSTRATIONS

LIST OF TABLES

SECTION I

INTRODUCTION

The thermoplastic (TP) modulator device is a leading candidate under development for real-time input of time-serial information in large time-bandwidth blocks into two-dimensional coherent optical processors (References 1 and 2). Serial input rates (bandwidth) of 100 MHz and higher, and time-bandwidth blocks of 10^6 or higher, are expected capabilities. Once this information has been established by the TP modulator in the input plane of the optical system, powerful parallel computations such as the Fourier Transform and Correlation functions can be carried out (Reference 3) essentially instantaneously on the entire block of data. These types of operations are difficult and costly to implement digitally and therefore this type of optical processing has potential to favorably impact Air Force applications such as synthetic aperture radar, Electronic Intelligence (ELINT), and terminal guidance which tend to require parallel processing of large data arrays. For the ELINT application, bandwidths of 100 MHz or higher are desirable due to the nature of the signals being analyzed.

The TP modulator is essentially a cathode ray tube (C.R.T.) device in which the phosphor face-plate has been replaced by a Thermoplastic-coated face-plate. Information is written onto the TP layer in form of charge patterns by a modulated scanning electron beam. Raster format is a typical scan pattern. The TP surface deforms in proportion to local charge density and this provides two-dimensional spatial phase modulation of a coherent beam passing through, or reflecting from, the TP layer. Stringent requirements apply to maintain acceptable optical quality of the faceplate and thermoplastic and also to the linearity and stability of the electron beam scan. Erasure and development of the TP layer is thermally controlled using the variations of viscosity, surface tension, and electrical resistivity with temperature.

Contract development of the TP modulator has resulted in laboratory breadboard achievement of a good basic performance level as follows (Reference 2):

Format: 1000 line by 1000 spots in 2.54 cm square (Raster scan)

Bandwidth: 70 MHz

Optical Quality: nearly ideal (i.e. diffraction limited)

Scan Quality: also nearly ideal as verified by Fourier plane spot characteristics

Having achieved good basic performance, attention has turned toward the remaining most serious development need which is frame cycling speed. At 100 MHz bandwidth, only 5 to 10 msec are required to fill the 10^6 element frame of the TP modulator. Presumably some additional time will be desired for downstream processing and read-out, so that total (frame) cycle times desired will be in the 20-100 msec range.

The current configuration of the Thermoplastic Modulator faceplate is illustrated in Figure 1. This configuration was designed with optical performance as the prime factor and with almost no attention to thermal aspects associated with repetitive write-develop-erase cycling. This emphasis was appropriate at the time of design. The fused silica substrate is a relatively poor thermal conductor and cooling is only by ambient air, with the possible addition of a radiative cooling effect. Single pulse transient heating data were taken for this configuration in air (i.e., no vacuum on thermoplastic side) (Reference 4). Decay times, for temperature on the thermoplastic side, of 100 to 200 msec were observed; with longer decay times corresponding to longer heating pulses. These times might be suitable for 10 pps operation, however, the experimental conditions are not appropriate, primarily the single pulse aspect. The single pulse case involves only the thermal diffusion of one burst of energy from the heating surface into the bulk of the substrate. which was initially at a uniform reference temperature. Under repetitive pulsed heating conditions, a heat build-up in the bulk of the substrate would be expected subject to the cooling conditions at the other (nonheated)

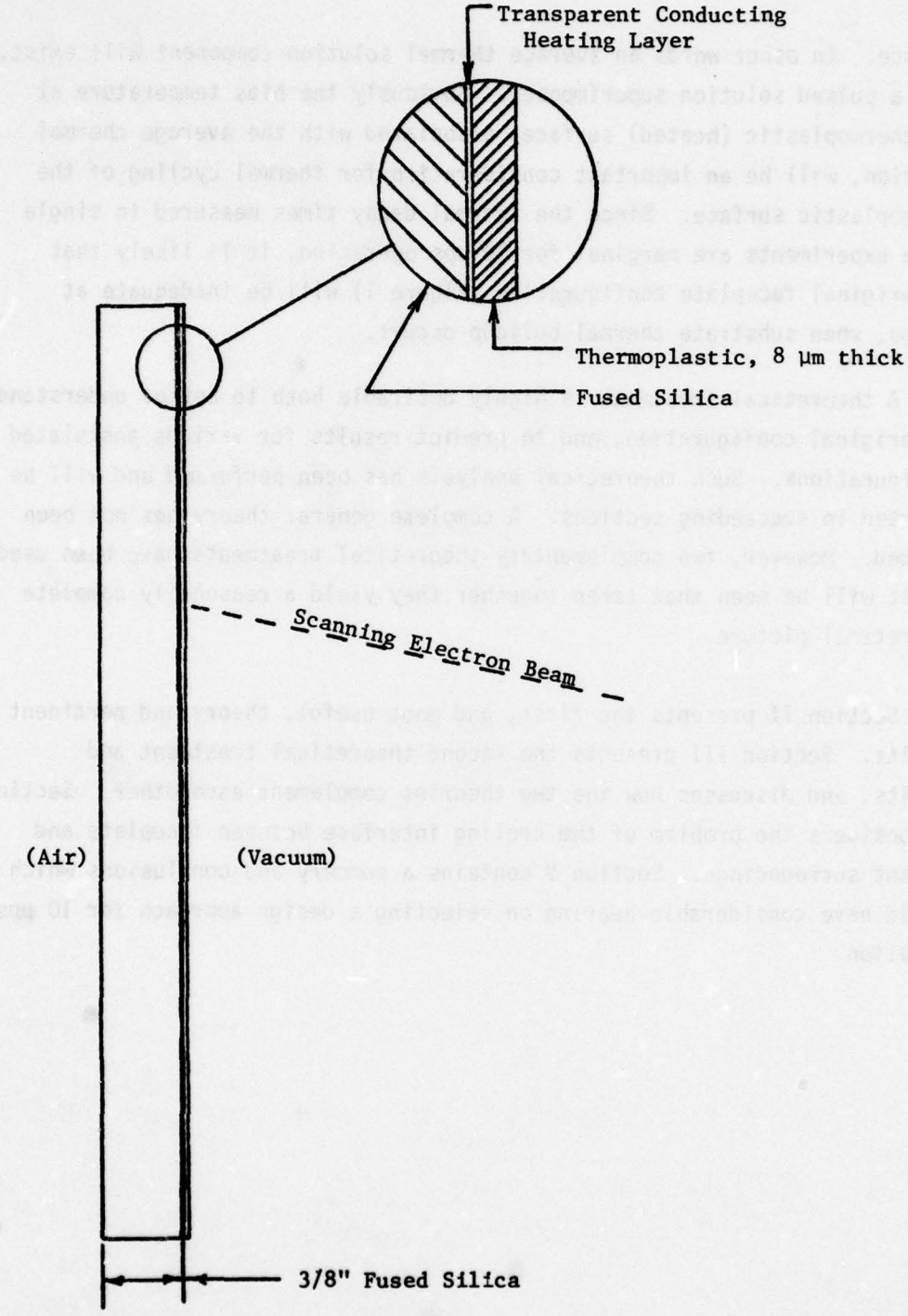

Figure 1. Current Thermoplastic Modulator Faceplate Configuration

surface. In other words an average thermal solution component will exist, with a pulsed solution superimposed. Obviously the bias temperature at the thermoplastic (heated) surface, associated with the average thermal solution, will be an important consideration for thermal cycling of the thermoplastic surface. Since the thermal decay times measured in single pulse experiments are marginal for 10 pps operation, it is likely that the original faceplate configuration (Figure 1) will be inadequate at 10 pps, when substrate thermal buildup occurs.

A theoretical treatment is highly desirable both to better understand the original configuration, and to predict results for various postulated configurations. Such theoretical analysis has been performed and will be reported in succeeding sections. A complete general theory has not been created. However, two complementary theoretical treatments have been used and it will be seen that taken together they yield a reasonably complete theoretical picture.

Section II presents the first, and most useful, theory and pertinent results. Section III presents the second theoretical treatment and results, and discusses how the two theories complement each other. Section IV considers the problem of the cooling interface between faceplate and ambient surroundings. Section V contains a summary and conclusions which should have considerable bearing on selecting a design approach for 10 pps operation.

SECTION II

REPETITIVE PULSED HEATING SOLUTION

This section presents the theory derived, and pertinent results obtained, for the case of repetitive pulsed heating. The geometry is that of a slab of thickness w which is maintained at a constant temperature ($\theta = 0$ for convenience) on one surface ($x = 0$) and insulated at the other surface ($x = w$), which is also the location of the heat source. This is expected to be a valid approximation to the case of a thermoplastic faceplate sufficiently cooled on the back side and with negligible radiative cooling from the vacuum (thermoplastic) side. An additional assumption is that a one-dimensional analysis is a valid approximation for the case stated (i.e., edge cooling is negligible compared with face cooling, and that there is no variation of other pertinent parameters across the faceplate). This analysis also will not account for the detailed sandwich structure of thermoplastic, heating, and sometimes other layers which actually exist at the heated surface of the substrate. These layers are relatively thin (circa 10 μm for example) and are intuitively expected to have a very minor effect on the thermal behavior. This aspect will be dealt with in some detail in Section III, to follow. The heat flow equation in the form applicable to this problem is (Reference 5):

$$\frac{\partial \theta}{\partial t} = D \frac{\partial^2 \theta}{\partial x^2} + \frac{Q}{\rho c}$$

where

$\theta = \theta(x,t)$ = temperature

t = time

x = distance

ρc = specific heat of substrate (per unit volume)

$D = k/\rho c$ = thermal diffusivity

k = thermal conductivity

$Q = Q(x,t)$ = heat source function

Boundary Conditions Are:

$$\theta\,(0,t) = 0$$

$$\left.\frac{\partial\theta}{\partial x}\right|_{x=w} = 0$$

The heat source function Q must be specified. A spatial dependence of $\delta\,(x-w)$ (where δ is the Dirac delta function) will be assumed and, initially, a time dependence of a semi-infinite train of delta functions: $\sum_{n=-\infty}^{0} \delta(t-nT)$. Where T is the heat pulse interval, and a solution valid for $t > 0$ is desired. Thus:

$$Q(x,t) = Q_0\,\delta\,(x-w) \sum_{n=-\infty}^{0} \delta\,(t-nT)$$

The assumed form of Q corresponds to heating at the thermoplastic surface and to a steady state pulsed condition, which will be approached asymptotically in practice at a time following startup equal to several thermal time constants of the slab.

For convenience, and to avoid any potential conceptual problems regarding the $\delta\,(x-w)$ function centered at a boundary surface, symmetry will be invoked to restate the problem in an extended x interval. A solution over the interval $0 \leq x \leq 4w$ will be sought with the boundary conditions:

$$\theta(o,t) = \theta\,(4w,t) = 0$$

A modified heat source function is required:

$$Q'(x,t) = 2Q_0\,[\delta(x-w) - \delta(x-3w)] \sum_{n=-\infty}^{0} \delta(t-nT)$$

Q' is changed in two ways. First, a negative heat source (or sink) has been located at x=3w equal in magnitude to the source at x=w. Inspection will verify that by symmetry this will result in $\theta(2w,t) = 0$; it then follows, also by symmetry, that $\frac{\partial\theta}{\partial x} = 0$ at x=w and x=3w. Thus, the desired physically reasonable boundary conditions result from the problem geometry and a form which will later be found convenient for solution has been achieved. Secondly, the magnitude of the heat source has been increased by the factor two. This is necessary also due to the symmetries of the new geometry. The delta function δ (x-w) is symmetric about x=w and thus, through its symmetric gradients $(\frac{\partial\theta}{\partial x})$, will drive equal heat flow components in both directions from x=w. The factor of two increase is needed to result in the desired heat flow (Q_o) into the solution region of interest $(0 \leq x \leq w)$. The solution approach is outlined as follows: Invoking linearity and time-space invariance, the source (driving) function Q (x,t) will be decomposed into a Fourier Sine series in x and the total solution expressed as a summation of component source solutions. The component solutions for time and space dependence will be found to be tractable. Thus expand:

$$\delta\ (x-w) - \delta\ (x-3w) = \sum_{n=1}^{\infty} c_n \text{ Sin } (\frac{\pi n x}{2w})$$

Standard procedures yield:

$$c_m = \frac{(-1)^{(\frac{m-1}{2})}}{w} \qquad (m \text{ odd})$$

$$c_m = 0 \qquad (m \text{ even})$$

or in terms of $n \equiv (m-1)/2$:

$$\delta\ (x-w) - \delta\ (x-3w) = \sum_{n=0}^{\infty} \frac{(-1)^n}{w} \text{ Sin } (\xi_n\ x)$$

where

$$\xi_n \equiv \frac{(2n+1)\pi}{2w}$$

Now assume a variables-separable solution for the nth component:

$$\theta_n(x,t) = f_n(t)\ \mathrm{Sin}\ (\xi_n\ x)$$

Substituting into the heat flow equation yields:

$$\frac{df_n}{dt} = -\xi_n^2\ D\ f_n + \frac{(-1)^n}{(w\rho c)} \cdot 2Q_o \sum_{m=-\infty}^{0} \delta(t-mT)$$

Again, linearity and time invariance are invoked. Component solutions for the nth term of the summation will be summed to obtain the total solution. These solutions are:

$$f_{nm} = \frac{(-1)^n}{(w\rho c)} \cdot 2Q_o e^{-D\xi_n^2\ (t-mT)} \quad (t \geq mT)$$

Summing over m yields:

$$f_n = \sum_{m=-\infty}^{0} f_{nm} = \frac{2Q_0(-1)^n}{w\rho c} \sum_{m=-\infty}^{0} e^{-D\xi_n^2\ (t-mT)} \qquad \text{(valid for } t \geq 0)$$

The m summation can be rewritten using $l = -m$ as:

$$e^{-D\xi_n^2 t} \sum_{\ell=0}^{\infty} e^{-\ell D\xi_n^2 T}$$

And the resulting summation can be recognized as the series of the form (Reference 6):

$$\left(\frac{1}{1-u}\right) = \sum_{i=0}^{\infty} (u)^i \qquad (|u| < 1)$$

where $u \equiv e^{-D\xi_n^2 T}$

Thus:

$$f_n = \frac{2Q_o(-1)^n}{(w\rho c)} \cdot \frac{e^{-D\xi_n^2 t}}{\left(1 - e^{-D\xi_n^2 T}\right)}$$

and the total solution is:

$$\theta(x,t) = \frac{2Q_o}{\rho c w} \sum_{n=0}^{\infty} \frac{(-1)^n e^{-D\xi_n^2 t}}{\left(1 - e^{-D\xi_n^2 T}\right)} \quad \text{Sin}(\xi_n X)$$

where (again):

$$\xi_n \equiv \frac{(2n+1)\pi}{2w}$$

This solution is valid for $0 \leq t \leq T$ and represents the steady state solution under pulsed conditions. The solution is also valid for $t > T$ is the heating source is considered to be turned off after the pulse at $t = 0$.

A major limitation of this treatment is the assumption of heating pulses which are delta functions in time. This is not physical and also may not be a valid approximation for cases of interest. Fortunately the solution derived can easily be extended to the case of rectangular heating pulses by again invoking linearity and time invariance conditions. The solution obtained is the system response function for $t \geq 0$ for an input function consisting of a train of delta functions extending from $t = 0$ to $t = -\infty$. A train of rectangular functions, the desired new input function, is the convolution of the original input function with one rectangle function. Thus, it follows from convolution algebra (Reference 7) that the desired new output function is the convolution of the rectangle function with the previous output function. The resulting solution, using

a rectangle function of unity amplitude and duration Δt starting at $t = 0$, is:

$$\theta = \frac{2Q_o}{(\Delta t\ kw)} \sum_{n=0}^{\infty} \frac{(-1)^n \left(e^{-D\xi_n^2 \Delta t} - 1\right) e^{-D\xi_n^2 t}}{\xi_n^2 \left(1 - e^{-D\xi_n^2 T}\right)} \text{ Sin } (\xi_n X) \quad (\Delta t \leq t \leq T)$$

where, again:

$$\xi_n \equiv \frac{(2n+1)\pi}{2w}$$

This solution still has an undesirable limitation, which is that it is valid only <u>between</u> heating pulses due to the limited region of validity of the prior solution for delta function heating pulses. This limitation can also be removed by further trickery based on linearity and time-invariance. Let $\theta\ (t, \Delta t, T)$ represent the solution just derived for a given time (t), pulse width (Δt) and period (T), with all other parameters considered fixed. A solution valid for $0 \leq t \leq \Delta t$ is desired. This solution may be obtained as the sum of two solutions of the form $\theta\ (t, \Delta t, T)$. Figure 2 illustrates how the appropriate input function (heating pulses) can be represented as the sum of two pulse trains:

$$Q(\tau) \propto \sum_{n=-\infty}^{0} \text{Rect}\left(\frac{\tau - nT}{t}\right) + \sum_{n=-\infty}^{-1} \text{Rect}\left(\frac{\tau - t - nT}{\Delta t - t}\right)$$

where, in this case:

$$\text{Rect } (u) = 1 \qquad 0 \leq u \leq 1$$
$$= 0 \qquad \text{otherwise}$$

The solution desired is the superposition of the responses to the two input pulse trains:

$$\theta = \theta\ (t,t,T) + \theta\ (T, \Delta t - t, T)$$

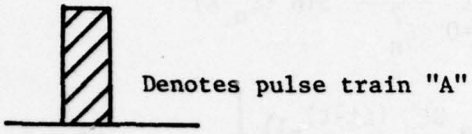

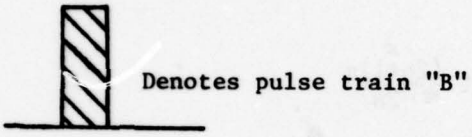

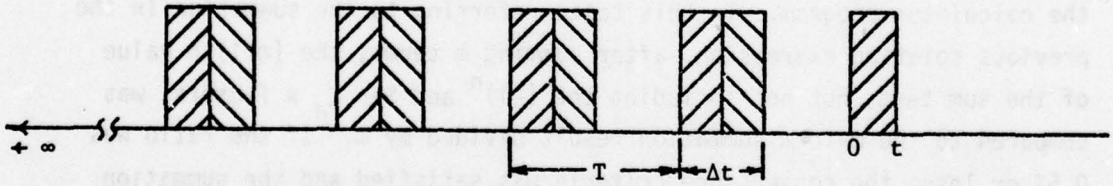

Desired heating pulse train= A+B

Figure 2. Superposition of Two Pulse Trains Extending to Minus Infinity to Yield Desired Heating Pulse Function

Or explicitly:

$$\theta(x,t) = \frac{2Q_o}{(\Delta tkw)} \sum_{n=0}^{\infty} \frac{(-1)^n}{\xi_n^2} \text{ Sin } (\xi_n X) \cdot$$

$$\cdot \left\{ \frac{(1-e^{-D\xi_n^2 t})}{(1-e^{-D\xi_n^2 T})} + \frac{(e^{D\xi_n^2 (\Delta t - t)} - 1)}{(e^{D\xi_n^2 T} - 1)} \right\} \qquad (0 \leq t \leq \Delta t)$$

And again:

$$\xi_n \equiv \frac{(2n+1)\pi}{2w}$$

This, combined with the previous solution valid outside the heating pulses, comprise a complete steady-state solution for the conditions assumed.

This solution was evaluated out to a finite number of terms using a Hewlett-Packard HP 9820 programmable desk calculator. Series convergence was verified by trial and error variation of the number of terms summed. In some cases over 1000 terms are needed to achieve an estimated accuracy of 0.5%. An ad hoc convergence test was formulated and incorporated into the calculator program. In this test, referring to the summation in the previous solution expression, after summing m terms, the (m+1)th value of the sum term, but not including the $(-1)^n$ and Sin ξ_n x factors, was compared to the m-term summation result divided by m. If the ratio was 0.5% or less, the convergence criteria was satisfied and the summation terminated. For some sets of values, only four terms were required for convergence. The calculator was programmed so as to plot temperature versus time for a specified position (x) and set of parameters (slab thickness, conductivity, etc.). Selected results are shown in Figures 3 and 5 thru 9, with all parameters noted on the graphs.

Figure 3 corresponds to the current configuration, with a 3/8" thick fused silica faceplate, except that the theory being plotted assumes "perfect" cooling on the back surface; a gross improvement over the air cooling of the current breadboard. The temperature scale shown corresponds to a heat input of 0.01 cal/cm^2 per pulse, or an average heating power of 0.419 watt/cm^2. Temperature values for other heating levels can easily be obtained by linear scaling. All cases to be discussed here are for x=0, i.e., the thermoplastic surface, because it is the thermal behavior of the thermoplastic which must be controlled. The results of Figure 3 will be interpreted relative to expected thermal cycling behavior requirements, after which the relevance of other results will more readily be apparent.

At least three necessary components of a complete temperature cycle for a thermoplastic can be identified:

(a) Erasure

(b) Recording (write & develop)

(c) Storage (read-out)

The three are listed in descending order of temperature required. For erasure the temperature must be held at a level high enough to allow charges to conduct through the thermoplastic and for a smooth surface to reform. The time required for erasure decreases with increasing temperature, however a rough estimate is that times on the order of a millisecond are required for temperatures in the 100 - 150°C range. For recording, a lower temperature is required, which will allow deformation but not too much charge leakage during the required recording interval, in this case 5-50 msec. Estimates of the temperature required for this case are in the 50-75°C range. For storage or readout, the temperature must be low enough to prevent significant charge leakage during the required interval, in this case 50-90 msec. Estimates of this temperature are also in the 50-75°C range. The astute reader has noticed that the temperature ranges estimated for record and readout are the same. This is not an error. Rather, it appears reasonable for the times involved, based on experimental observations (Reference 8) of develop and erase

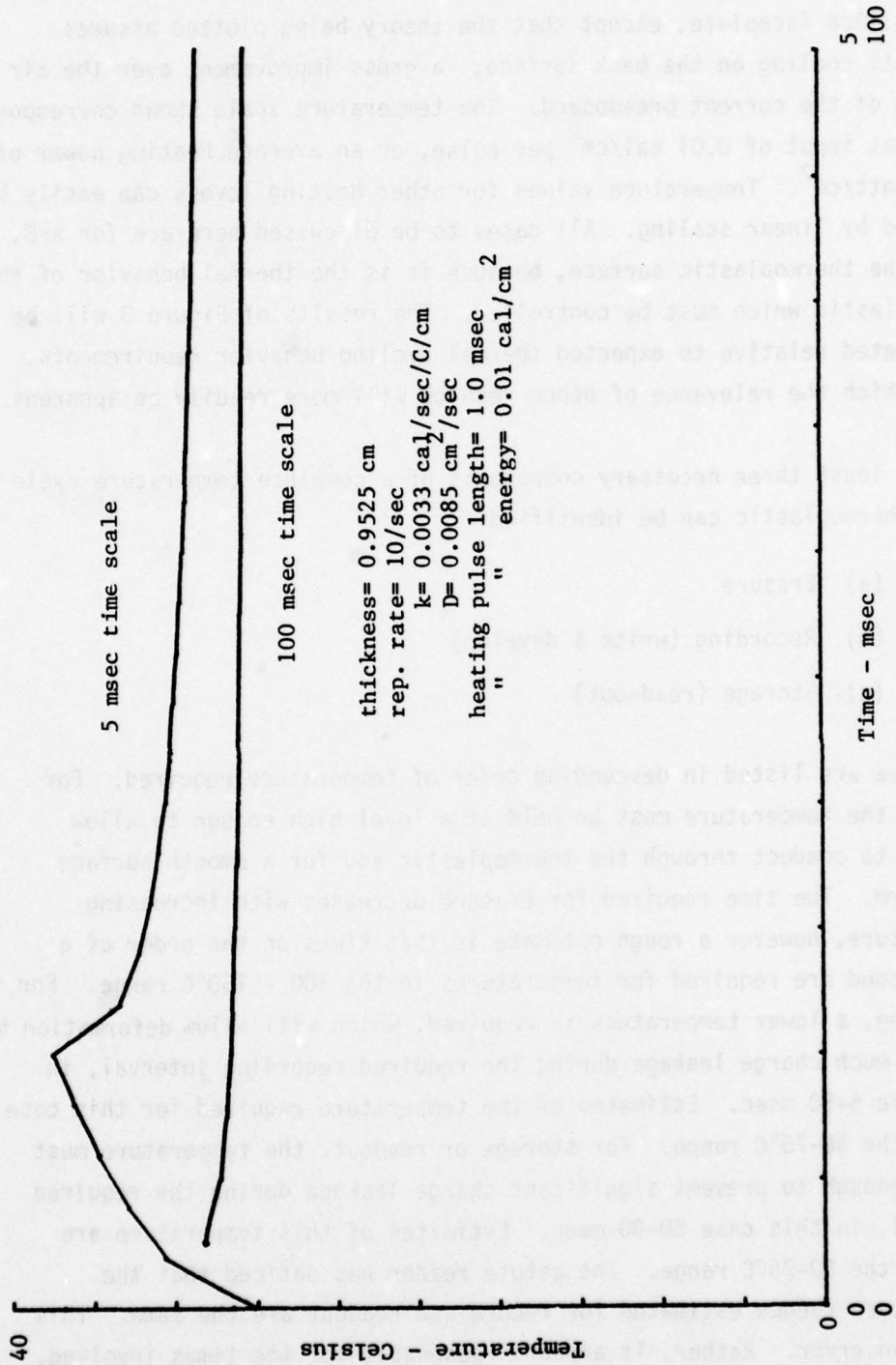

Figure 3. Heated Surface Temperature Variation for 3/8" Fused Silica Substrate

times which occur when the thermoplastic is held at a constant temperature. For example, at 49°C, the diffraction from a written grating peaked after 40 seconds then took 150 seconds to decay to 13% of peak value. This implies that develop rates are several times faster than erase rates at fixed temperatures. Of course, higher temperatures would be required to yield the desired develop times. However, it seems reasonable to expect that similar behavior will prevail since several distinct physical processes are involved. The speed of development is believed to be governed primarily by physical properties (e.g., surface tension and viscosity) while erasure is determined primarily by electrical resistivity. As verified by the experimental results at 49°C temperature, the physical and electrical processes proceed at their own distinct rates.

A strategy for achieving proper record-erase cycling with the simple type of temperature history illustrated in Figure 3 can now be suggested as diagrammed in Figure 4. The times shown are representative rather than specific. A heating pulse lasting perhaps one millisecond and sufficient to result in erasure, must be followed by a cooling interval prior to writing. (Otherwide, newly written charges would be conducted away too quickly.) The "write" time interval is determined by the data rate and format, and 10 msec is a typical value for 100 MHz operation. After a sufficient "develop" time interval, readout can occur. An obvious potential problem is that the temperature during readout is not much lower than during development. Thus, there will be some droop of readout optical signal during the readout period. This effect can be minimized by using the smallest possible readout interval, the largest possible develop time interval, and establishing the minimum average develop temperature required to allow acceptable diffraction efficiency to be reached.

Temperature from the theory is plotted relative to the temperature maintained at the cooled surface. If forced liquid cooling is used, a reasonable value of the reference temperature would be 2°C. Referring to Figure 3, for erasure a temperature peak circa 100°C or above is desired. Using linear scaling the temperature during record and readout phases is approximately 75°C, which is much too high. Heat input per

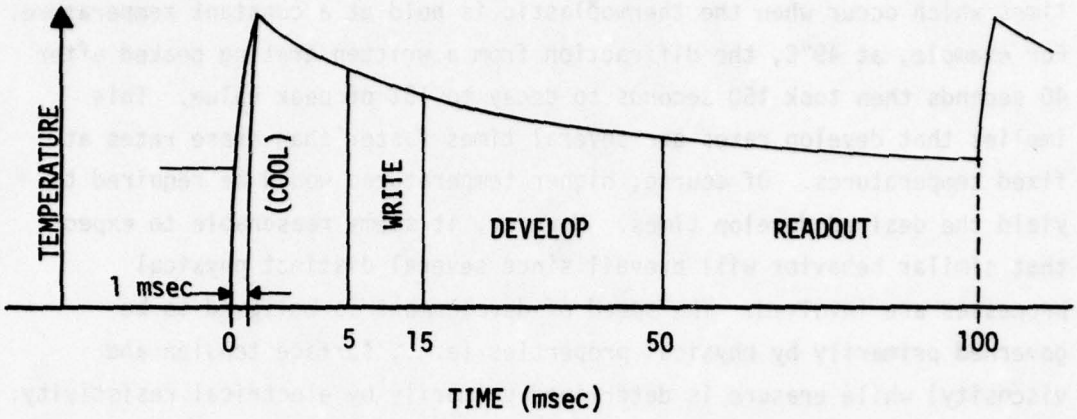

Figure 4. Possible Strategy for Record-Erase Cycling with Simple Temperature History

pulse may be varied but the shape of the curve is not affected and thus the ratio of erase and record temperatures is constant (relative to cooled-surface reference temperature). Obviously, this configuration is not good. To ease comparison of results, a figure of merit (R_t) is defined; the ratio of the temperature value which is exceeded for one millisecond to that existing at 10 milliseconds following initiation of a one millisecond heating pulse. For the case already discussed R_t is only 1.14, whereas an R_t of about 2.0 is probably required for a cooled-surface temperature of 2°C. To achieve values of 50°C and 100°C for the two temperatures used in defining R_t (i.e., recording and erase temperatures) would require a cooled surface temperature near -300°C, with obvious attendant physical problems. Figure 5 gives theoretical results for a silica substrate with a reduced thickness of 4 mm. For this case, R_t = 1.32, much better but still nowhere near sufficient. The required cooled-surface temperature would be about -100°C. A thickness of 4 mm approaches the minimum worthy of consideration due to mechanical considerations. The substrate must withstand the vacuum pressure differential and must be rigid enough to maintain a good optical surface.

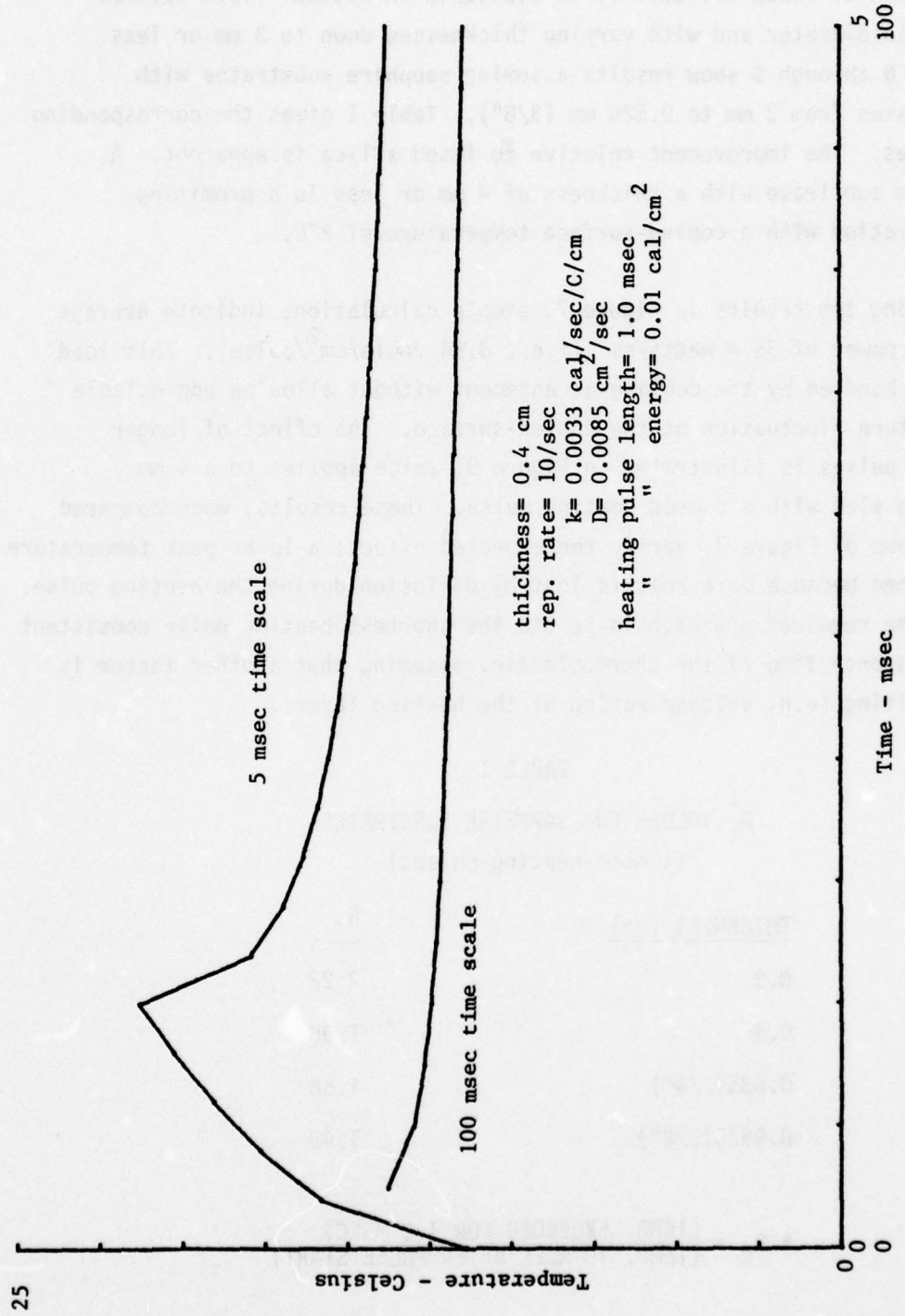

Figure 5. Heated Surface Temperature Variation for 4 mm Fused Silica Substrate

Sapphire is a crystalline material with thermal conductivity many times that of fused silica. It is available in optical flats several inches in diameter and with varying thicknesses down to 3 mm or less. Figures 6 through 9 show results assuming sapphire substrates with thicknesses from 3 mm to 9.525 mm (3/8"). Table I gives the corresponding R_t values. The improvement relative to fused silica is apparent. A sapphire substrate with a thickness of 4 mm or less is a promising configuration with a cooled-surface temperature of 2°C.

Using the results in Figure 7, simple calculations indicate average heating power of 35.4 watts/cm^2 (i.e., 3.54 Joule/cm^2/pulse). This load must be handled by the cooling arrangement without allowing appreciable temperature fluctuation at the cooled-surface. The effect of longer heating pulses is illustrated in Figure 9, which applies to a 4 mm sapphire slab with a 5 msec heating pulse. These results, when compared with those of Figure 7, verify the expected effect; a lower peak temperature is reached because more heat is lost by diffusion during the heating pulse. Thus, the required approach is to use the shortest heating pulse consistent with response time of the thermoplastic, assuming that another factor is not limiting (e.g. voltage rating of the heating layer.)

TABLE I

R_t^* VALUES FOR SAPPHIRE SUBSTRATES
(1 msec heating pulses)

THICKNESS (cm)	R_t
0.3	2.22
0.4	1.96
0.635(1/4")	1.68
0.9525(3/8")	1.48

$$* R_t = \frac{\text{(TEMP. EXCEEDED FOR 1.0 MSEC)}}{\text{(TEMP. 10 MSEC AFTER PULSE START)}}$$

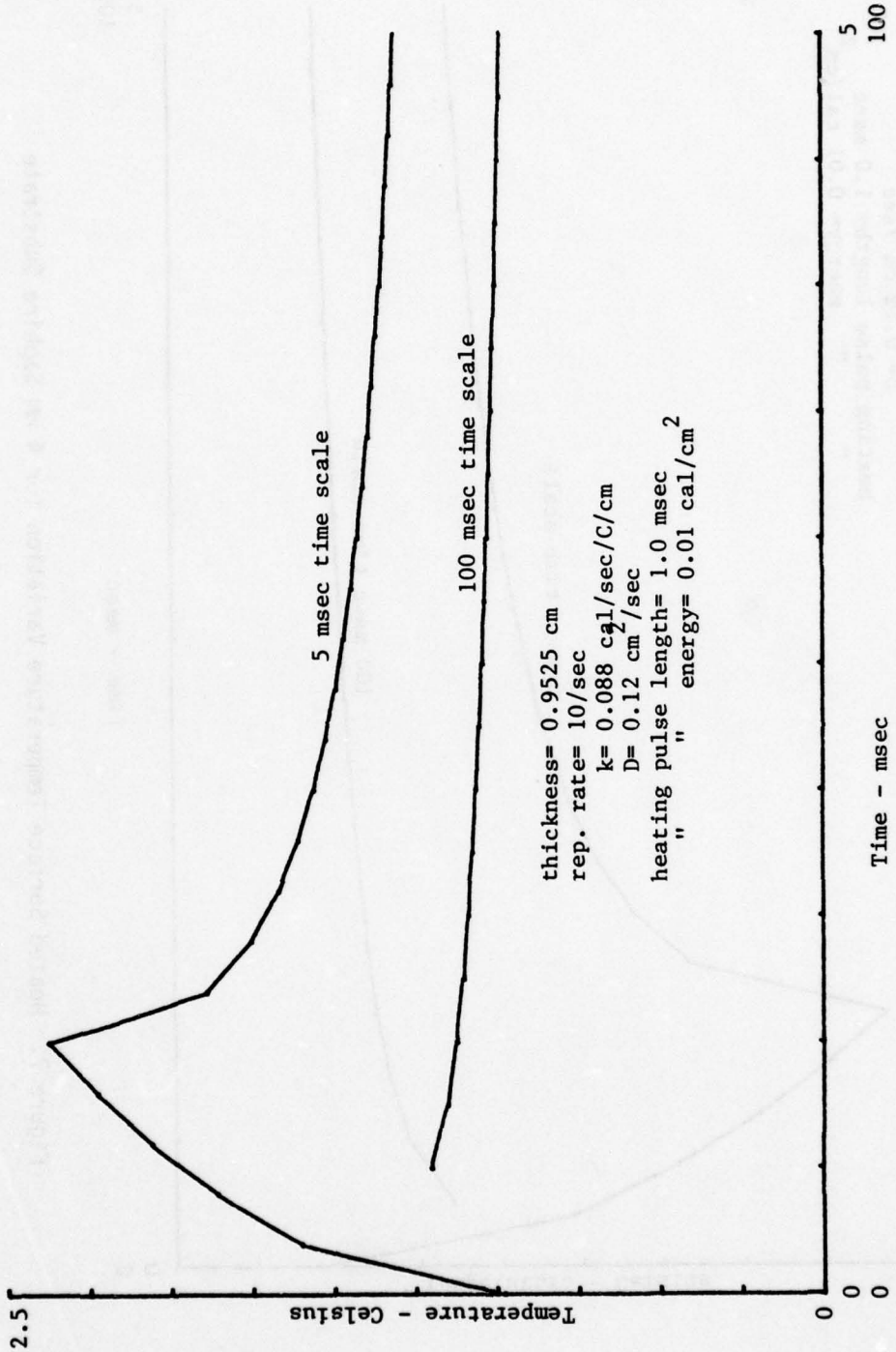

Figure 6. Heated Surface Temperature Variation for 3/8" Sapphire Substrate

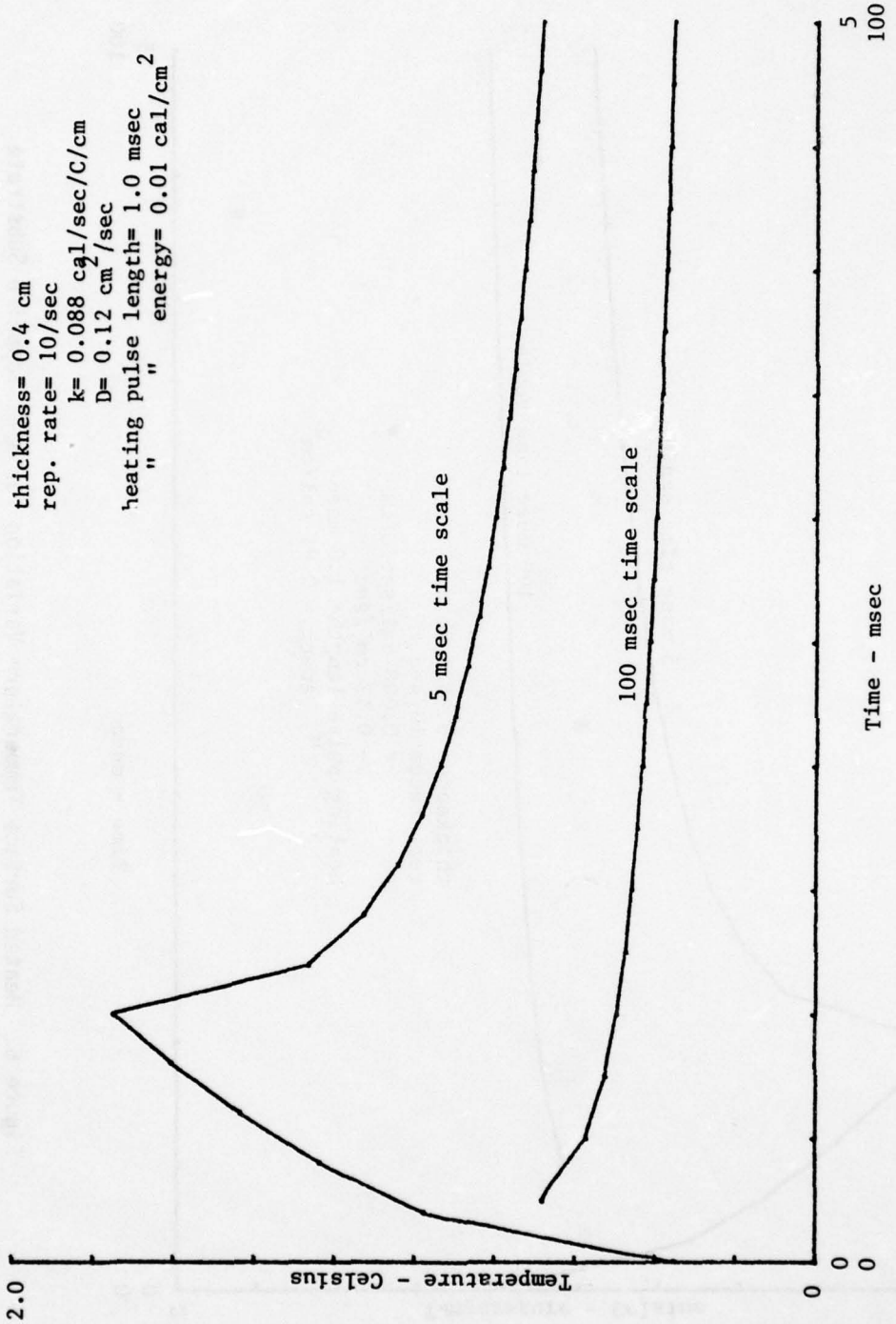

Figure 7. Heated Surface Temperature Variation for 4 mm Saphire Substrate

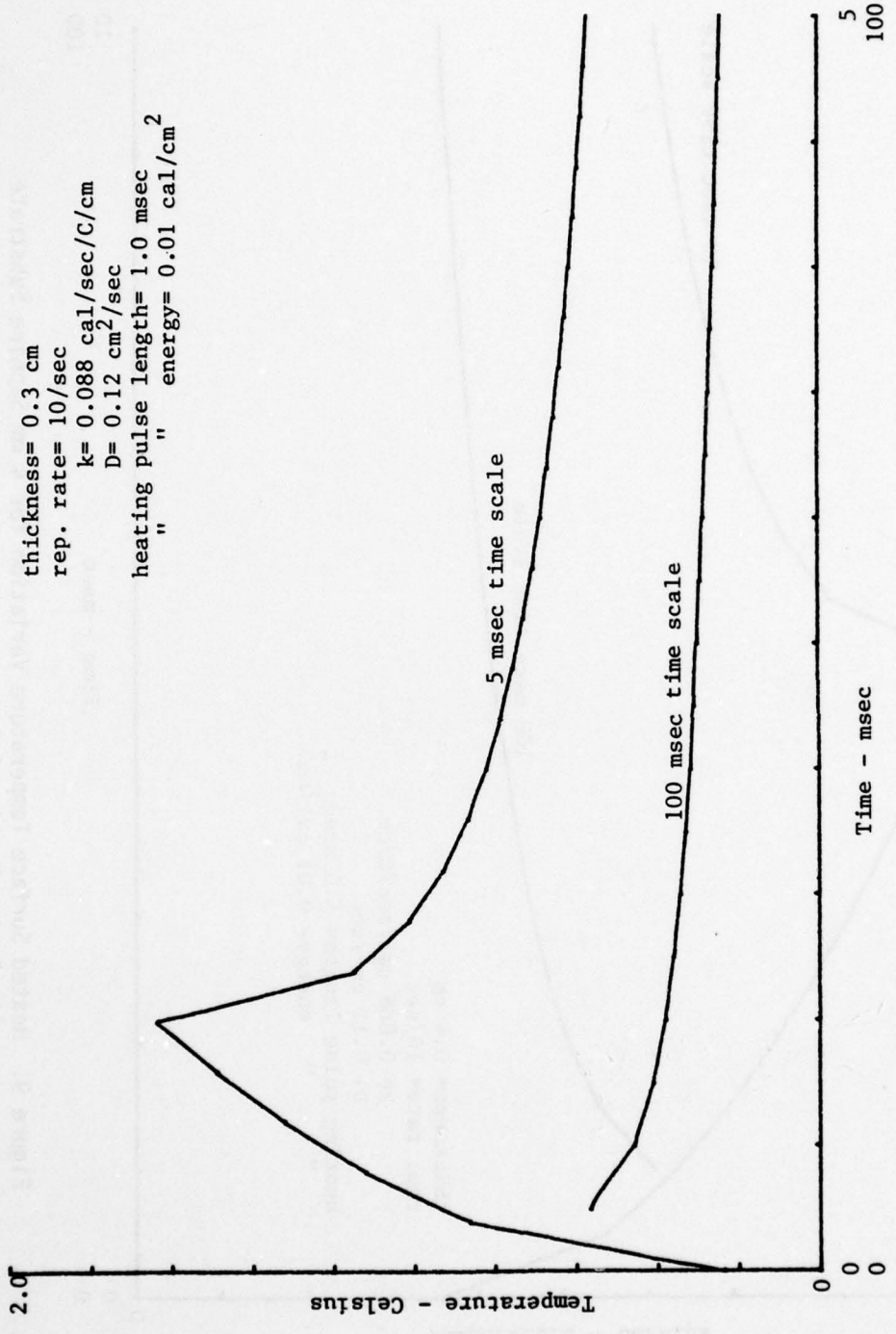

Figure 8. Heated Surface Temperature Variation for 3 mm Saphire Substrate

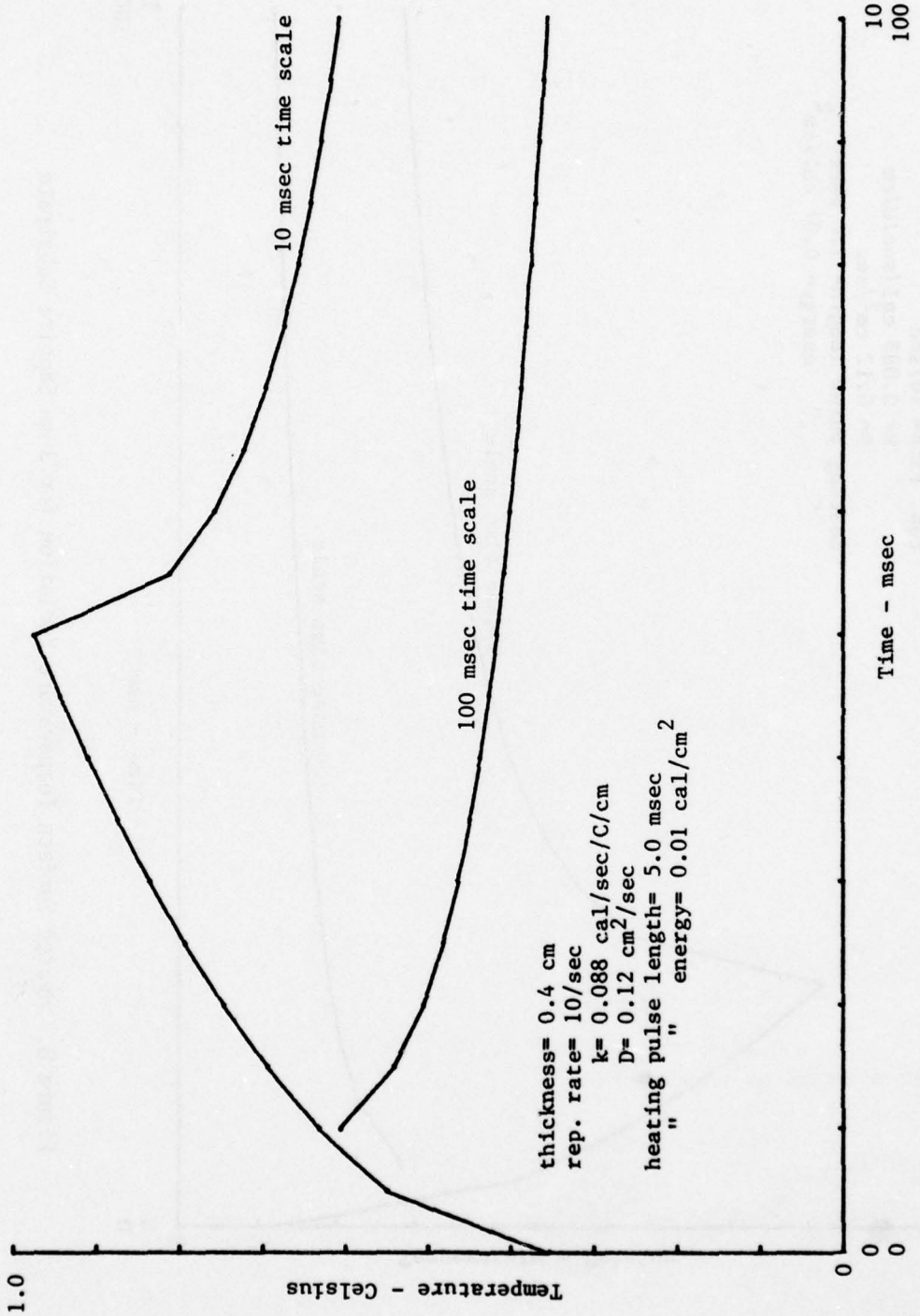

Figure 9. Heated Surface Temperature Variation for 4 mm Saphire Substrate with 5 msec Heating Pulse

SECTION III

SURFACE THERMAL TRANSIENT ANALYSIS

As mentioned, the slab analysis in the previous section does not account for details of thermal bahavior associated with the thin sandwich structure at the thermoplastic surface. As a minimum of complexity, there is a layer of thermoplastic, typically about 8 μm thick, and a transparent conductive layer between the thermoplastic layer and the substrate slab. Heat is generated in the conductive layer and must diffuse into the thermoplastic layer. This takes a finite time and meanwhile heat also is diffusing into the substrate slab.

An intuitive analysis of the situation might be as follows: The thermoplastic layer is very much thinner than the substrate slab for any practical case and should not appreciably affect the thermal behavior of the slab. Therefore, the slab analysis of the previous section should describe thermal behavior of the slab face under the thermoplastic reasonably well. The thermoplastic layer temperature should follow substrate temperature but with a delay approximately equal to the thermal time constant of the thermoplastic layer. The thermal time constant for a slab of thickness T is defined (Reference 9):

$$\tau_o = \frac{T^2}{\pi^2 D}$$

Where $D \equiv \frac{k}{\rho c}$ = thermal diffusivity

A measured value for D is not available for the thermoplastics used. However a brief survey of values available for some similar plastics indicates that the following are representative:

$k = (2 \cdot 10^{-4})$ cal-sec^{-1}-°C^{-1}-cm^{-1}

$c = .33$ cal-°C^{-1}-g^{-1}

$\rho = 1$ g - cm^{-3}

Thus

$$D = \frac{k}{\rho c} \simeq 6 \cdot 10^{-4} \ \text{cm}^2 - \text{sec}^{-1}$$

And, for 8 μm thickness:

$$\tau_o = 108 \ \mu\text{sec}$$

Thus, a delay on the order of 100 μsec is indicated. When considering heating pulse lengths of one millisecond or longer, such a delay seems insignificant. The thermal conductivity (and diffusivity) of the thermoplastic is about an order of magnitude lower than that of even the poorest substrate (Fused Silica). Thus, during the heating pulse a major portion of the heat must be flowing into the substrate rather than the thermoplastic. The impact of this effect is hard to predict although it seems unfavorable. In order to gain a more accurate measure of these effects, a computer simulation approach was implemented to model thermal behavior in the vicinity of the thermoplastic layer for the times during and immediately following the heating pulse. Although this treatment, like the previous one, is not completely general, it will be found that very little interpretation is required to bridge the gap between the two, resulting in a reasonably complete theoretical understanding.

In essence the computer simulation involved setting up a one-dimensional space grid (line array of points) of temperature values in and near the thermoplastic layer and then letting the temperatures evolve thru finite time steps as governed by a finite difference version of the basic partial differential equation for heat transfer:

$$\frac{\partial \theta}{\partial t} = D \frac{\partial^2 \theta}{\partial x^2} + \left(\frac{1}{\rho c}\right) Q$$

Where

θ = temperature

D = thermal diffusivity

ρc = specific heat (per unit volume)

Q = heat source function

The corresponding finite difference equation is:

$$\frac{(\theta_{i,j+1} - \theta_{i,j})}{\Delta t} = \frac{D}{h^2}(\theta_{i+1,j} + \theta_{i-1,j} - 2\theta_{i,j}) + \frac{Q_{i,j}}{\rho c}$$

Where:

Δt = time step

h = Space grid spacing

$\theta_{i,j}$ = temperature at i^{th} grid position at j^{th} time step

$Q_{i,j}$ = heat source function value at i^{th} grid position at j^{th} time step

The solution typically used a space grid including 10 points thru the thermoplastic layer and 90 points extending into the substrate slab. More points would be desirable but practical solution times were a limiting factor. Assuming a typical value for thermoplastic thickness, 8 μm, the solution region extended only 72 μm into the substrate region, while typical substrate thicknesses range from 3,000 μm to 10,000 μm. This obviously imposes limitations on the validity of the solution, which in this case amounted to a maximum solution time, as will be discussed later. It should be noted that the finite difference equations use the appropriate distinct property values (e.g., D, ρ, c) in the respective media. Also, appropriately modified equations must be used to account for boundary conditions at the thermoplastic face and the interface between thermoplastic and substrate. An artificial boundary condition was also needed to terminate the space grid where it (un-physically) ended in the substrate. The boundary conditions will be discussed and the actual equation used will be given but not derived. To a large degree, the form used is intuitively obvious. At the thermoplastic face, the boundary condition applied was zero heat flux (i.e., $\frac{\partial \theta}{\partial x} = 0$). The resulting modified equation is:

$$\theta_{o,j+1} = \theta_{o,j} + \frac{D\Delta t}{h^2}(\theta_{i,j} - \theta_{o,j})$$

where, i=0 has been set at this face. The interface boundary is somewhat more complex. Heat generation was assumed to occur in an infinitesimally thin region located at this interface. This assumption may be questionable since any conductive heating layer will have finite thickness. However, if the layer is typically metallic, it will have thermal conductivity much higher than the adjacent media and intuitively would be expected to behave "thermally thin." The equation used at the interface (i=c) was:

$$\theta_{c,j+1} = \theta_{c,j} + \frac{2\Delta t}{h^2(k_1/D_1 + k_2/D_2)} \cdot \left\{ k_1 \left(\theta_{c-1,j} - \theta_{c,j}\right) + \ldots \right.$$

$$\left. \ldots + k_2 \left(\theta_{c+1,j} - \theta_{c,j}\right) + h\, Q_{c,j} \right\}$$

Where subscripts 1 and 2 denote thermoplastic and substrate values, respectively. At grid end, the boundary condition θ=o was imposed. Obviously no boundary condition would be correct, so the simplest was chosen.

Initial conditions were zero temperature everywhere. The heating source ($Q_{c,j}$) was "turned on" at t=0($\approx$j) and kept on at a constant value for the number of j (time) increments corresponding to the selected heating pulse length. Solution procedure consisted of repetitively using the jth time step temperature values to calculate the (j+1)th values. A stability criterion involving the choice of time step size must be satisfied:

$$2D\Delta t < h^2$$

Physically this criterion amounts to assuring that excessive heat flow is not allowed in one time interval due to using too large a time step. Otherwise, negative temperatures and associated oscillations can occur. Intuition suggests that for better solution accuracy, the inequality should be satisfied strongly. Then fractional temperature changes per time step will be small at most grid positions. In the actual cases to be reported here, the inequality was satisfied by ratios of 7.5 and 2.1 for silica and sapphire substrates, respectively. The small ratio for sapphire was chosen due to practical solution time considerations.

Detailed discussion of the expected impact of two key limitations of this solution approach is in order; first, the limited space grid size and the resulting arbitrarily assigned zero-temperature boundary condition at grid end. The general nature of the solutions is that a "blob" of heat grows at the plastic-substrate interface during the heating pulse and immediately begins spreading into the plastic and substrate, in the normal manner of a diffusion process. For a finite time, no appreciable heat has reached the depth corresponding to the end of the grid. It seems reasonable to expect that, during this time, conditions at or beyond grid end have not affected the solution. This rationale was used as a guide to judge the time interval over which a given solution could be trusted. Secondly, the zero temperature initial condition is not realistic for steady state pulsed heating conditions, as was seen in the previous section. However, using linearity, this solution can be superimposed on the residual temperature solution from all previous pulses to yield a complete solution. Actually, the expected properties of said residual solution are such as to justify it being considered essentially a constant temperature (in space and time) relative to the rapid spatial and temporal variations of the present transient solution.

Solution was implemented on a Hewlett-Packard 9820 Programmable Desk Calculator. An internal check was incorporated in the form of a sub-program which, at selected solution time intervals, summed the total heat existing in solution space. This was to be compared to the known input pulse heat energy. Discrepancies of more than 2-3% were suspect. (Perfect agreement probably should not be expected due to the finite difference approximation involved). In addition, a test case was performed which simulated the response of a uniform medium to a delta function one dimension in time and space heating pulse. The closed form (Gaussian) solution for this case is well known, and simulation results were in good agreement.

The first case simulated was an 8 μm thermoplastic layer on a fused silica substrate. The values used for material parameters here and for the sapphire substrate were:

	Thermoplastic	Silica	Sapphire
k(Thermal Cond., cal-sec^{-1}°C^{-1}-cm^{-1}	0.0002	0.0033	0.088
D(Thermal Diffusivity, cm^2 -sec^{-1})	0.0006	0.0085	0.12

Time steps of 50 nsec and a total heating pulse energy of 0.01 Cal/cm^2, were used in all cases to be reported. Figure 10 gives the results using a 100 μsec heating pulse. Results are plotted only to a depth of six times TP layer thickness, although the solution grid extended to 10 times TP thickness. At times of 500 μsec and later, temperature values near grid end began to exceed 1% of maximum. Also, at 500 μsec 97.8% of total input heat was accounted for in the grid, while at 900 μsec only 90.1% remained. Obviously, the artificial boundary condition at grid end is beginning to affect results sometime after 500 μsec. Note that the temperature profile across the TP layer becomes roughly level after 300 to 400 μsec. (i.e., 200 to 300 μsec after pulse end.) This is in agreement with the 100 μsec TP slab time calculated previously. From 500 μsec on, the TP temperature roughly follows the interface temperature, remaining somewhat higher or, equivalently, somewhat delayed. Thus, these results verify the intuitive expectations discussed.

Figure 11 shows a combination of results from this simulation and the steady-state slab theory of the previous section. Three different temperatures were derived from the simulation results shown in Figure 10, including average temperature in the TP layer and plotted versus time. Also plotted is the surface temperature from the steady-state solution of Section II for the same case, except that a bias level has been substracted. The value substracted is the residual temperature which exists in the steady-state solution after one pulse interval, (0.1 sec). It is apparent that the two theories tend to join near 500 μsec solution time for this particular case. Thus, the two treatments are complementary and together comprise a reasonably general theoretical understanding.

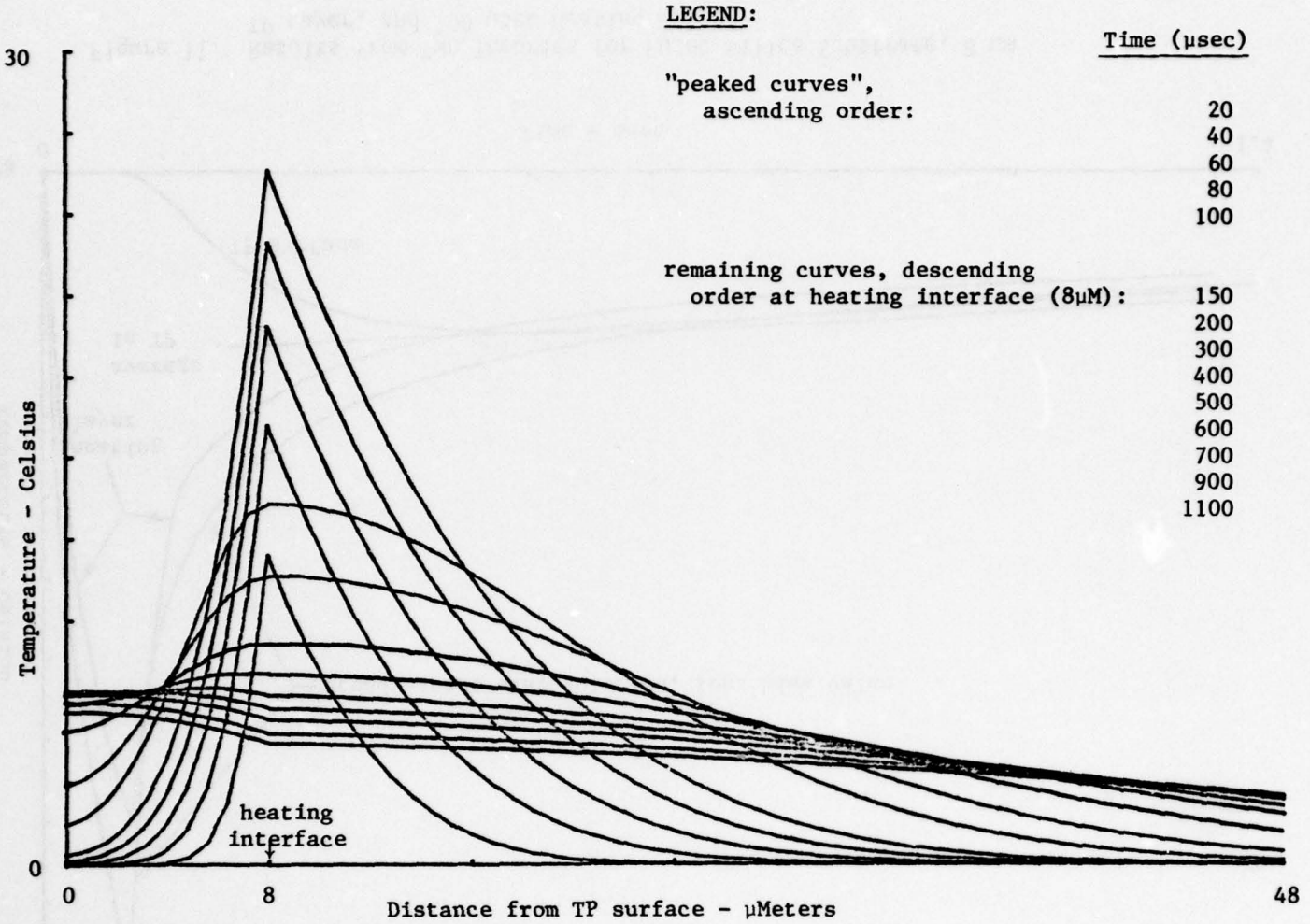

Figure 10. Temperature Variations in 8 μmeter TP Layer on Fused Silica Substrate with 100 μsec Heating Pulse

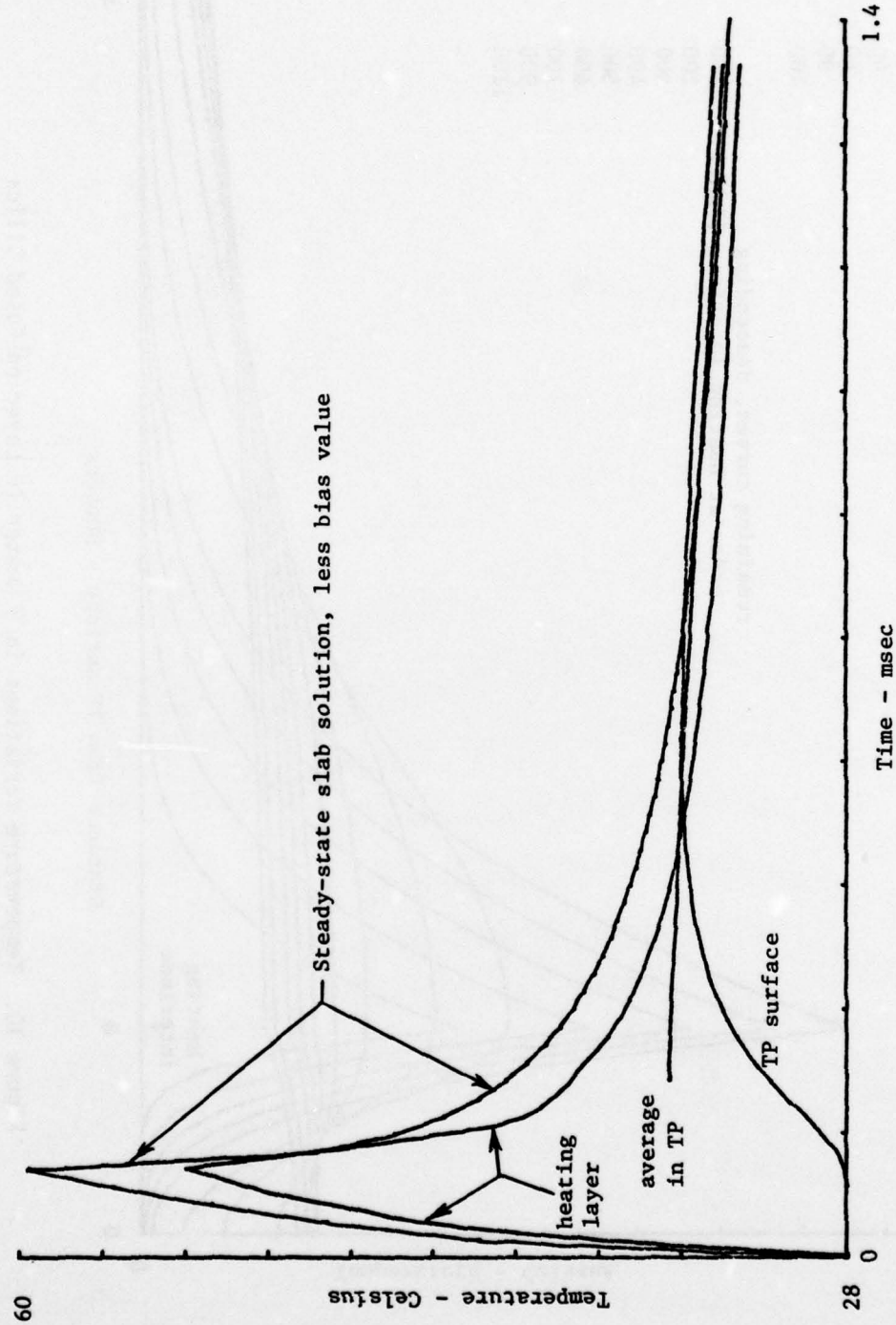

Figure 11. Results from Two Theories for Fused Silica Substrate, 8 μm TP Layer, and 100 μsec Heating Pulse

Simulation results for an 8 μm TP layer on a sapphire substrate using a 100 μsec heating pulse are shown in Figure 12. In order to satisfy the Δt stability criterion by just a factor of two, because of the higher thermal conductivity of sapphire, it was necessary to increase h, resulting in only five grid points through the TP layer. The other alternative, reducing Δt, would have resulted in unacceptably long running times. Another problem is also apparent from the results. Also, due to the higher thermal conductivity of sapphire, the simulation becomes suspect after shorter solution times in the silica substrate case. Heat is diffusing faster into the substrate. Just at the end of the heating pulse (100 μsec) only 91.2% of the input heat energy is accounted for in the solution grid. Thus, the results should be interpreted intuitively rather than quantitatively. The same basic behavior found in the silica substrate case is apparent. TP layer temperature lags substrate temperature by roughly the slab thermal time constant of the TP layer: About 100 μsec as previously calculated for 8 μm TP.

In summary, the simulations have not revealed basic information beyond what could be guessed intuitively. They have at least verified intuitive expectations in detail. Obviously this simulation technique could, with minor modifications, handle additional layers such as the heating layer or a protective coating.

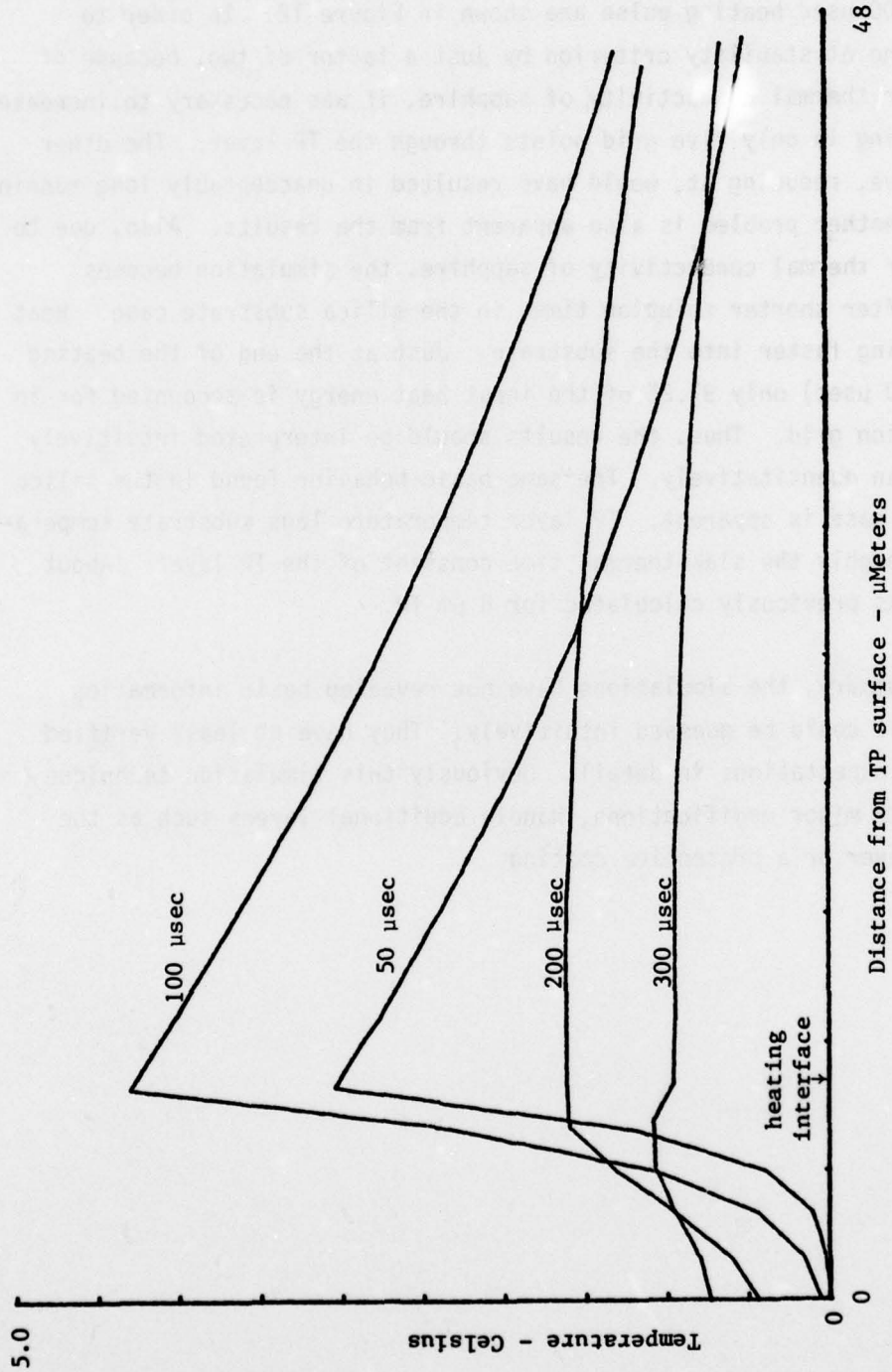

Figure 12. Temperature Variations in 8 µm TP Layer on Sapphire Substrace with 100 µsec Heating Pulse

SECTION IV

COOLING CONSIDERATIONS

Previous sections have been concerned with thermal aspects within the thermoplastic layer and substrate. The average heat load deposited must be dumped into the ambient environment while maintaining acceptable temperatures at the cooled substrate surface. For the likely case of a 4 mm thick sapphire substrate, this cooling load was calculated in Section II and is 35.4 Watts/cm^2 or 228.4 Watts for a 1 inch square area. Previous considerations have assumed a 2°C cooling temperature. These parameters define a critical cooling problem as will be verified. This section will report design analysis results for both laminar and turbulent flow liquid (water) cooling and will discuss the possibility of thermoelectric cooling.

1. LAMINAR FLOW COOLING

A design analysis for laminar flow cooling will be summarized here. Well known equations were used and they and pertinent references are given in the Appendix.

For laminar cooling a thin channel is formed between parallel plates, one of which is the cooled surface of the substrate. Water flows between these plates with an assumed entrance temperature near 0°C. The basic goal may be described as follows: To achieve a required minimum value of heat transfer coefficient with acceptable flow and pressure drop. The heat transfer coefficient is defined:

$$h = \frac{Q}{A\Delta\theta}$$

where

h = heat transfer coefficient

Q = heat flow across surface

A = surface area

$\Delta\theta$ = Temperature differential from surface to average coolant temperature

Based on computer simulations performed by ERIM (Reference 10), h=2 Cal/sec/cm^2/°C is required to keep surface temperature fluctuations down to one degree or less. In terms of the average heat flow for the 4 mm sapphire case (Q = 8.5 cal/sec/cm^2), this implies a coolant film temperature drop of 4.25°C. This is more than ideally desired, but probably is acceptable.

In laminar flow, the value of h is determined solely by the geometry and the coolant thermal conductivity (See Appendix). For water and this geometry, a channel spacing of 0.839 mil (0.0213 mm) is required for h=2. A minimum average flow velocity is required to maintain an acceptable coolant temperature rise along the channel. Using 5°C as the maximum acceptable rise, an average flow velocity of 1690 cm/sec is calculated. For a 1 inch (2.54 cm) long channel, the required flow pressure drop is calculated as 1,787 psi (12.32 x 10^8 dynes/cm^2). This is obviously an unworkable pressure (over 100 Atm.) considering mechanical strength alone.

Very little latitude exists (i.e., parametric tradeoffs) for reducing the flow pressure for the Laminar case by the required factor of 100 or so. Thus, the Laminar case is ruled out.

2. TURBULENT FLOW COOLING

Turbulent Flow cooling offers a better chance for success than the laminar case since the heat transfer coefficient is dependent on factors in addition to the geometry and coolant thermal conductivity. Again, design results will be summarized. The well known equations and references used will be found in Appendix. The geometry is the same slit between parallel plates as used for the laminar flow case.

Using the material properties of water, the following parametric equations were developed (See Appendix):

$$\Delta P = \frac{6.9274 \cdot 10^{-6} \, (Re)^{1.8}}{a^3}$$

$$h = \frac{3.4761 \cdot 10^{-5} \, (Re)^{0.8}}{a}$$

where:

ΔP = pressure drop for 1 inch (2.54 cm) long channel-dynes/cm^2

h = coolant heat transfer coefficient, cal/cm^2/°C/sec

Re = Reynolds Number of flow (dimensionless)

a = coolant channel spacing - cm

The remainder of the design procedure involves choosing a trial Reynolds number and using the second relationship to calculate the value of a required for h=2. Then the first equation is used to calculate ΔP. Results are:

Re	10^4	10^5	$2 \cdot 10^5$
a(mils)	10.8	68.4	120
ΔP(psi)	76.2	19.1	12.6

Re values of 10^5 and above yield potentially acceptable results. The (average) flow velocity for Re = 10^5 is calculated to be $4.43 \cdot 10^3$ cm/sec which corresponds to a total flow (for a 1 inch wide channel) of 31 gal/min (1.96 liter/sec). This seems a large flow and brings up the question of the power dissipated in the flow itself, which is calculated at 258 Watts (i.e., more than the cooling load.). Fortunately, almost all this power is dissipated as viscous heating distributed within the bulk of the flowing coolant and thus does not add to the heat load which must be conducted across the coolant surface film with coefficient h. This heating does add to the coolant temperature rise from channel entrance to exit. However, this increase is calculated to be only 0.03°C and is insignificant. Both pressure drops and bulk (viscous) coolant heating in the coolant lines and other cooling system components must be considered in the specification of the coolant pump and heat exchanger.

This analysis indicates that a reasonable turbulent flow cooling design may be possible. Possible areas of uncertainty which remain include entrance effects on both pressure drop and cooling coefficient (See Appendix)

and the potential dynamic distortion of the thermoplastic surface driven by turbulent flow vibrations.

3. THERMOELECTRIC COOLING

TE cooling has obvious attraction compared with fluid cooling. Literature for several commercially available TE cooler modules was reviewed. Some pertinent characteristics are tabulated:

	Cambion 3958-01	MELCOR CP2-31-06L
Cooling area dim(cm)	$(3.175)^2$	$(3.0)^2$
ΔT max (°C)	65	67.5
Qc max (T_H = 27°C) Watts	16.6	30
Cooling Flux at Q_c max(Watts/cm^2)	1.65	3.33

ΔT_{max} is the temperature drop which can be maintained with zero cooling load, while Qc max is the cooling load achievable with zero ΔT, both defined at maximum permissible current through the module, and at a hot surface temperature (T_H) of 27°C. An approximately straight line connecting these two points on a temperature-versus-cooling-load graph defines the performance of the module at maximum current and with the hot surface temperature held at 27°C. Cooling capacity decreases for lower currents and with lower hot surface temperatures. Thus, for example, a module can simultaneously handle both 0.5 Qc_{max} and 0.5 ΔT_{max}. In any case, it is obvious that such modules fall far short of the cooling flux densities required for the sapphire substrate case (circa 35 Watts/cm^2).

Another approach is to use a glass substrate in hopes that lower heat flux (resulting from lower substrate thermal conductivity) will enable TE cooling. In this case, as shown in Section II, a cooling temperature circa -100°C must be maintained in order to achieve desired TP surface temperature variations and the cooling flux is about 5 watts/cm^2. The cooling flux is still greater than the maximum achievable by the best of the two modules with zero temperature drop.

Based on the above analysis, thermoelectric cooling is ruled out of further consideration.

SECTION V

SUMMARY AND CONCLUSIONS

A theoretical understanding, based on two complementary treatments, has been achieved with regard to the thermal behavior of thermoplastic face-plate structures. Temperature variations in the TP layer and substrate slab can be predicted. The effects of important variables such as heating pulse duration, thermoplastic layer thickness, substrate thickness, etc., can now be studied. The theory was applied to silica and sapphire substrates and furnished results to substantiate the following conclusions:

1. A simple silica substrate design is not feasible for 10 pps operation (essentially because of too low a value of thermal diffusivity), unless cooled-surface temperatures of -100°C can be considered.

2. Sapphire substrates of 4 mm thickness or less are thermally acceptable for 10 pps operation with cooled surface temperatures near 0°C. With a 4 mm slab, an average heat flux of about 35 watts/cm^2 is predicted.

3. For heating pulse lengths of 1 msec or longer, as probably will be required due to TP response time, the temperature response of the TP layer may be expected to be essentially that of the surface of an uncoated substrate. Transient effects on a 100 μsec time scale occur in the TP layer, in agreement with simple slab thermal time constant calculations.

Laminar and turbulent flow water cooling, and thermoelectric cooling were considered for the face-plate-to-ambient interface. Analysis indicated that laminar flow cooling is totally out of the question, while a turbulent flow design may be feasible. Success of the turbulent approach is not assured and the design will be very critical. Perhaps the use of a different coolant and even direct refrigeration would yield a less marginal design. These were not investigated. Thermoelectric cooling does not appear feasible due to the heat loads involved, which are much greater than the capabilities specified for commercially available units.

APPENDIX A

LIQUID COOLING EQUATIONS

The following three references were used and will be referenced by number within this appendix:

A-1. Kutateladze, S. S. and V. M. Borishanskii, "A Concise Encyclopedia of Heat Transfer," Pergamon Press, New York, 1966. (1st English edition, translated by J. B. Arthur, edited by W. Cohen).

A-2. Rohsenow, W. M. and H. Choi, "Heat, Mass and Momentum Transfer," Prentice-Hall, Inc., Englewood Cliffs, N. J., 1961.

A-3. McAdams, William H., "Heat Transmission," Third Edition, McGraw-Hill Book Co., Inc., New York, N. Y., 1954.

1. LAMINAR FLOW

a. Pressure Drop

From p. 334, Reference A-1 and pp 57-64, Reference A-2

The friction factor, $f = \frac{\Delta P}{2(L/D)\rho V^2} = \frac{24}{Re}$

Where:

ΔP = pressure drop

L = channel length

D = equivalent diameter = $2a$

a = channel spacing

ρ = density

V = velocity

Re = Reynolds number = $\frac{DV}{\nu}$

ν = kinematic viscosity

For water: $\nu = 1.5405 \cdot 10^{-2}$, cm^2/sec

$\rho = 1$ g/cm^2

b. Heat Transfer

From p. 106, Reference A-1

For flat slit of thickness a:

$Nu = 7.60$ for $PeD/L \leq 70$

Where Pe = Peclet number = $VD/(k/\rho c)$

and Nu = Nusselt number = $hD/k = \frac{2ha}{k}$

Where

$k/\rho c$ = thermal diffusivity

h = film heat transfer coefficient

For a slit with one insulating wall: Nu = 5.8

Slightly different values of Nu are given for different geometries and different boundary conditions. Nu = 6 was used for calculations given in this report.

c. Temperature Rise Along Flow

The equation used, which can be derived from basic heat flow balance considerations, is:

$$V = \frac{Q}{\rho cab\Delta T}$$

2. TURBULENT FLOW COOLING

a. Pressure Drop

From Reference A-1; p. 334, Reference A-2, p. 59 and Reference A-3; p. 155, empirical correlations for the friction factor are:

$$f \cong \frac{0.0791}{(Re)^{0.25}} \quad (5 \cdot 10^3 \leq Re \leq 5 \cdot 10^4)$$

$$f \cong \frac{0.046}{(Re)^{0.2}} \quad (5 \cdot 10^4 \leq Re \leq 2 \cdot 10^5)$$

These are applicable to circular pipes, but from Reference A-1; p 334, Reference A-2; p. 62; and Reference A-3; p. 157: For noncircular cross-sections use same correlations but use the equivalent hydraulic diameter De (=2a for our case) in calculating Re.

Page 72 of Reference A-2 gives a graph of f vs L/D, (i.e., entrance effect), for turbulent entry flow. There is an increase in overall f which is less than a factor of two for $L/D \geq 4$.

b. Heat Transfer Coefficient

From Reference A-1; p. 110, Reference A-2; p. 192, and Reference A-3; pp 219-20, there are two accepted correlations for the heat transfer coefficient:

$$Nu = \frac{hD}{k} = \frac{2ha}{k} = 0.023(Re)^{0.8}(Pr)^{0.4}$$

(and)

$$\frac{h}{c\rho V}\ (P_r)^{2/3} = \frac{0.023}{(Re)^{0.2}}$$

where:

$$Pr \equiv \text{Prandtl Number} = \frac{\nu}{(k/\rho c)} = 11.5 \text{ for this case}$$

Both relationships are for circular pipes and are valid for $L/D \geq 50$, $Re \geq 5 \cdot 10^3$ and $P_r \gtrsim 1$. Though they have different forms, they yield results which are comparable within acceptable correlation accuracy (i. e., 30% maximum error). By arbitrary choice, the second relationship was used for calculations. Discussion of modifications for the noncircular case may be found in Reference A-1; p. 113 and Reference A-3; p. 242. Depending upon exact geometry and other variables, various forms are given. All are either identical to one of the above relationships, or differ only by 30% or less. Since the reference material is somewhat ambiguous concerning our particular geometry, no modification was applied in our calculations.

It will be noted that the turbulent flow design results far from satisy the condition $L/D \geq 50$ given for the heat transfer coefficient correlations. Thus, significant entrance effects could occur.

These are discussed in Reference A-3, pp 224-6, and Reference A-2, p. 195. Reference A-3 suggests the following correction factor for the heat transfer coefficient:

$$1 + (D/_L)^{0.7}$$

Thus, entrance effects are seen to enhance heat transfer. For the design results in this report the enhancement is of the order of 25%. In general, the turbulence condition of the entering flow has a very strong effect on heat transfer and pressure drop. The correlations used are valid only for fully developed turbulence conditions. This must be considered in the design of the cooling system and features such as turbulence generating vanes or such may be needed at channel entrance.

REFERENCES

1. Currie, G. D. et. al., "The ERIM TOPR in Optical Data Processing", in the Proceedings of the SPIE 20th Anniversary Technical Symposium, Vol. 83, August 23-27, 1976, San Diego, California.

2. I. Cindrich et al., Real-Time Optical Data Modulator, AFAL-TR-75-77, Air Force Avionics Laboratory, Wright-Patterson AFB, Ohio, May 1975.

3. Vanderlugt, A., Proc. IEEE, 62, 1300 (1974).

4. I. Cindrich, et al, Real-Time Modulator for Coherent Optical Processing, pp 99-104, AFAL-TR-73-88, Air Force Avionics Laboratory, Wright-Patterson AFB, Ohio, May 1973.

5. Carslaw, H. S. and J. C. Jaeger, Conduction of Heat in Solids, 2nd Ed., Oxford University Press, Fair Lawn, N. J., (1959).

6. Burington, R. S., Handbook of Mathematical Tables and Formulas, 3rd Ed., p. 44, Handbook Publishers, Inc., Sandusky, Ohio (1957).

7. Mason, S. J. and H. J. Zimmermann, Electronic Circuits, Signals, and Systems, p. 326, Wiley, New York (1960).

8. D. Flannery, Private communication based on experiments performed at the Air Force Avionics Laboratory, Wright-Patterson AFB, Ohio in 1976.

9. Hildebrand, F. B., Advanced Calculus for Applications, pp. 449-51, Prentice-Hall, Englewood Cliffs, N. J. (1962). Note: Although the problem treated in this reference is that of a rod with insulated sides, the mathematics are obviously identical to those of a slab with no transverse variations. The slab time constant is from the slowest decaying term in the transient solution given.

10. Colburn, W. S., Private communication based on computer simulations performed at the Environmental Institute of Michigan, under contract to the Air Force Avionics Laboratory in September, 1977.

*U.S.Government Printing Office: 1978 — 657-002/246